Mixed-Doped Lithium Nickel Vanadate As Cathode Material By Wet Chemistry And Polymer Precursor Method

Leena Ismail[1], S.Ramesh[2], Tan Winie[3] and A.K. Arof[1,*]
[1]*Physics Department, Faculty of Science, University of Malaya (UM), 50603 Kuala Lumpur, Malaysia*

[2]*Faculty of Applied Science, MARA University of Technology, 40450 Shah Alam, Selangor, Malaysia*

[3]*Faculty of Engineering and Science, Universiti Tunku Abdul Rahman, 53300 Setapak, Kuala Lumpur, Malaysia*

*Corresponding Author: *akarof@um.edu.my*

Abstract

The mix doped $LiNi_{1-x}Mn_xVO_4$ (0 « x « 1) have been synthesized by using soft chemistry and polymer precursor method. XRD, TGA/DTGA and SEM analysis have been carried out to study the structural and physical properties of the samples as cathode material for lithium ion batteries. Citric acid was added during the sample preparation as the chelating agent. SEM images showed that the grain size of the composite sample increased as the temperature was increased. The prepared samples have been characterized thermally by TGA/DTGA results.

Keywords: mix-doped, $LiNi_{1-x}Mn_xVO_4$, wet chemistry, polymer precursor method

1. INTRODUCTION

The inverse spinel lithium transition metal compound such as $LiNiVO_4$, $LiCoVO_4$ and $LiMnVO_4$ have been studies due to their high cell voltage for lithium ion batteries. The conventional solid state reaction method has the disadvantages of high temperature requirement for preparation, bigger crystallite size and time consuming. Soft chemistry which is also known as solution precipitation technique (sol gel) and polymer precursor method is an alternative method which can improve the structure and the electrochemical performance of the prepared cathode. The mixed-doped composite does not change the structure of the inverse spinel structure but may increase the material kinetics in terms of cycle life and the capacity performance [1]. The polymerization that occurs during the addition of citric acid and polymer may distribute metal ions through the polymeric chain [2]. Addition of polymeric source results in the reduction of particle size of the prepared sample in the nanocrystalline powder [2]. Generally the inverse spinel cathode material such as $LiNiVO_4$ exhibits low capacity compared to the theoretical value of 148 mAh g^{-1}. Subramania et al. [3] in 2006 has demonstrated the cathode capacity of 102 mAh g^{-1} by combustion technique. This result was comparable to Kalyani et al. [4] that obtained 90 mAh g^{-1} of their initial charge discharge studies in 2002.

2. EXPERIMENTAL TECHNIQUE

Cathode materials of $LiNi_{1-x}Mn_xVO_4$ ($0 \leq x \leq 1$) were prepared using the sol- gel and polymer precursor method. Lithium acetate dihydrate, $LiCH_3COO.2H_2O$ (Fluka), nickel acetate tetrahydrate $Ni(CH_3COO)_2.4H_2O$ (Ajax Chemicals), $Mn(CH_3COO)_2.4H_2O$ (Aldrich) and ammonium metavanadate NH_4VO_3 (Ajax Finechem) were dissolved in distilled

water to prepare the $LiNi_{1-x}Mn_xVO_4$ ($0 \leq x \leq 1$). To prepare the $LiNi_{1-x}Mn_xVO_4$ ($0 \leq x \leq 1$), required amounts of manganese acetate tetrahydrate $Mn(CH_3COO)_2.4H_2O$ (Aldrich) were mixed with the $LiCH_3COO.2H_2O$: Ni $(CH_3COO)_2.4H_2O$: NH_4VO_3 (1:1:1) dissolved in distilled water.

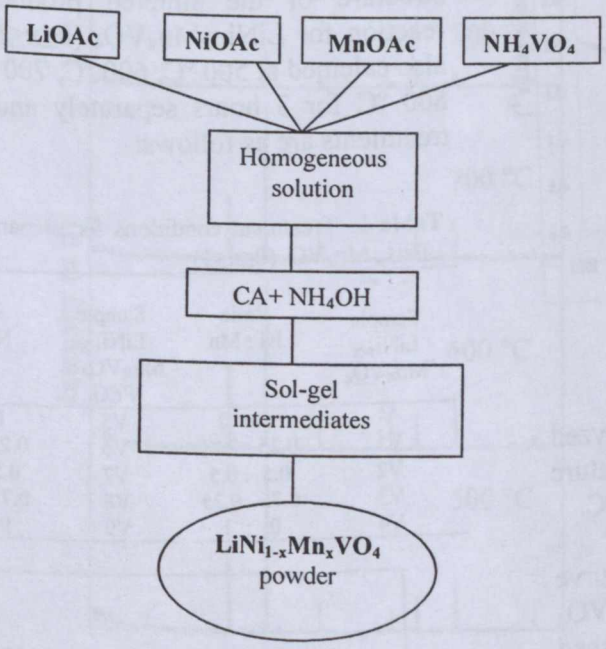

These two solutions were further stirred with constant heating until homogeneous. Then the citric acid and ammonium hydroxide, NH_4OH solutions were added into the homogeneous mixture until a gas evolution was observed. The citric acid acts as the complex agent and helps the improvement in electronic conductivity of the prepared cathode [5]. After the occurrence of gas evolution, a dark blue dry gel was formed. The gel obtained was further heated to form a loose powder called as a precursor. The precursor was then sintered at various temperatures ranging from 500 °C to 800 °C for 3 hours.

3. RESULTS AND DISCUSSION

3.1 Reaction Steps Equations

The possible reaction steps involved in the preparation of $LiNi_{1-x}Mn_xVO_4$ (1), (2), (3), (4), (5); $LiNi_{1-x}Mn_xVO_4$ + PEG (1), (2a), (3), (4a), (5) in this work are as follows:

V_2O_5 begins to form when NH_4VO_3 reacted with citric acid $C_6H_8O_7$ in the mixture:

$$2NH_4VO_3 + 2C_6H_8O_7 \rightarrow V_2O_5 + 2(NH_4)C_6H_7O_7 + H_2O \quad (1)$$

A gas will evolve from $LiCH_3COO.2H_2O$, $Ni(CH_3COO)_2$ and $Mn(CH_3COO)_2$ reaction with $C_6H_8O_7$. As the result, the CO_2 gas and $LiNi_{1-X}Mn_XC_6H_5O_7$ were produced:

$$LiCH_3COO + (1-X)Ni(CH_3COO)_2 + XMn(CH_3COO)_2 + C_6H_8O_7 + 9O_2 \rightarrow LiNi_{1-X}Mn_XC_6H_5O_7 + 10CO_2 + 8H_2O \quad (2)$$

$$LiCH_3COO + (1-X)\ Ni(CH_3COO)_2 + XMn(CH_3COO)_2 + HO(C_2H_4O)nH + C_6H_8O_7 + 9O_2 \rightarrow LiNi_{1-X}Mn_XC_6H_5O_7 + (C_2H_4O)n + 10CO_2 + 9H_2O$$

$$LiNi_{1-X}Mn_XC_6H_5O_7 + (C_2H_4O)n + 6CO_2 + H_2O \rightarrow LiNi_{1-X}Mn_XC_6H_5O_7 + CO_2 + H_2O \quad (2a)$$

V_2O_5 may be oxidized by $C_6H_8O_7$ because it is an oxidant in acidic solution. The V(V) in V_2O_5 can be reduced to V(IV) with the gas evolution and forms $(VO)^{2+}$ ion. $(NH_4)(VO)\ C_6H_5O_7$ will be produced when the $(VO)^{2+}$ ion was then reacted with $(NH_4)\ C_6H_7O_7$:

$$V_2O_5 + C_6H_8O_7 + 2(NH_4)C_6H_7O_7 + 4O_2 \rightarrow 2(NH_4)(VO)C_6H_5O_7 + 6CO_2 + 6H_2O \quad (3)$$

From the Eqs. (1) - (3), the total reaction equation would be as follows:

$$2NH_4VO_3 + 4C_6H_8O_7 + LiCH_3COO + (1-X)\ Ni(CH_3COO)_2 + XMn(CH_3COO)_2 + 13O_2 \rightarrow LiNi_{1-X}Mn_XC_6H_5O_7 + 2(NH_4)(VO)C_6H_5O_7 + 15H_2O + 16CO_2 \quad (4)$$

$$2NH_4VO_3 + 4C_6H_8O_7 + LiCH_3COO + (1-X)\ Ni(CH_3COO)_2 + XMn(CH_3COO)_2 + HO(C_2H_4O)nH + 13O_2 \rightarrow LiNi_{1-}$$

$_xMn_xC_6H_5O_7 + 2(NH_4)(VO)C_6H_5O_7 + 8 H_2O + 7CO_2$ (4a)

3.2 TGA/DTGA Studies

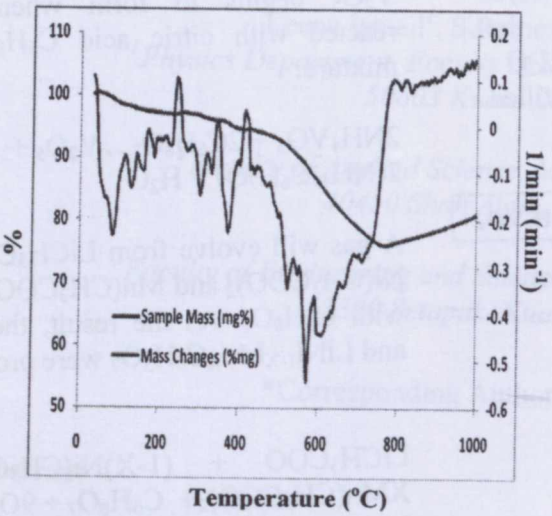

Fig. 1 TGA/DTGA curve of the precursor

The TGA and DTGA curve was analyzed for the dried precursor in the temperature range from room temperature to 1000 °C.

Fig. 1 show the TGA and DTGA curve analyzed for the dried $LiNi_{1-x}Mn_xVO_4$ precursor. H_2O and lithium acetate finished to evaporate with 3.07% before 100 °C. Citric acid and ammonium metavanadate start to decompose in the temperature ranged from100 °C to 200 °C while manganese acetate decomposed at above 300 °C. Three main endothermic peaks in temperature range from 80 °C to 600 °C located at 80 °C, 371 °C, and 573 °C respectively. For both results, gasses such as H_2O and CO_2 were gradually reduced. In order to obtain the stable vanadate, the residuals formed will continue to react after the decomposition process [6].

This reaction will cause the weight loss of the compound. The TGA spectra have also been analyzed to elucidate the mechanism for the synthesis of $LiNi_{1-x}Mn_xVO_4$. Based on the proposed total decomposition equation in air atmosphere, the calculated value of the total weight loss of the decomposition process is 65.9%.

$4LiNi_{1-x}Mn_xC_6H_5O_7.(VO).(NH_4)\ C_6H_5O_7 + 37O_2 \rightarrow 4LiNi_{1-x}Mn_xVO_4 + 48CO_2 + 22H_2O + 4NH_3$ (5)

3.3 XRD Characterization

X- ray diffraction analysis was carried ou to determine the phases and the crysta structure of the sintered product. Th reaction for $LiNi_{1-x}Mn_xVO_4$ ($0 \le x \le 1$) wer also calcined at 500 °C, 600 °C, 700 °C an 800 °C for 3 hours separately and thos treatments are as follows:

Table 1 Treatment conditions for preparation o $LiNi_{1-x}Mn_xVO_4$ ($0 \le x \le 1$)

Sample $LiNi_{1-x}Mn_xVO_4$	Ratio Ni : Mn	Sample $LiNi_{1-x}Mn_xVO_4$ + PEG	Ratio Ni : Mn
V	1 : 0	V5	1 : 0
V1	0.25 : 0.75	V6	0.25 : 0.75
V2	0.5 : 0.5	V7	0.5 : 0.5
V3	0.75 : 0.25	V8	0.75 : 0.25
V4	0 : 1	V9	0 : 1

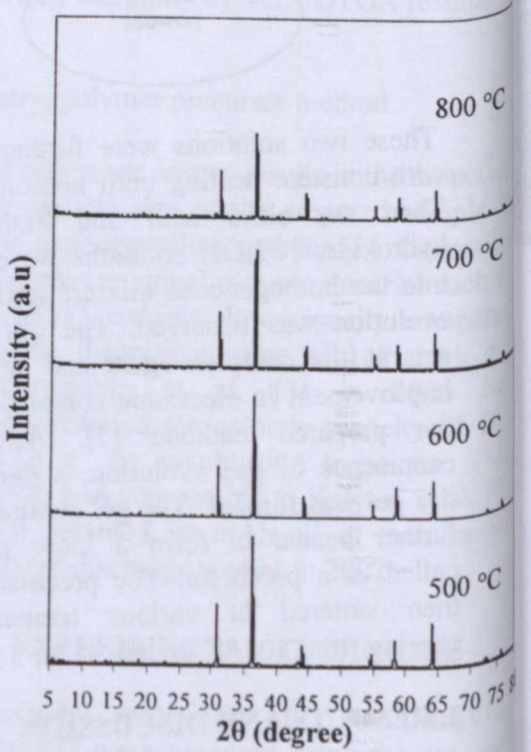

Fig 2 XRD Pattern of V calcined at various temperatures

Fig. 2 shows that the XRD analysis for the final product when the powder was sintered at 500 °C for 3h, small impurities amounts of NiO was identified by powder XRD. The observed peaks for NiO are near 37.3°, 43.3° and 62.9° [7]. The single phase of V was observed starting from sample treated at 600 °C to 800 °C.

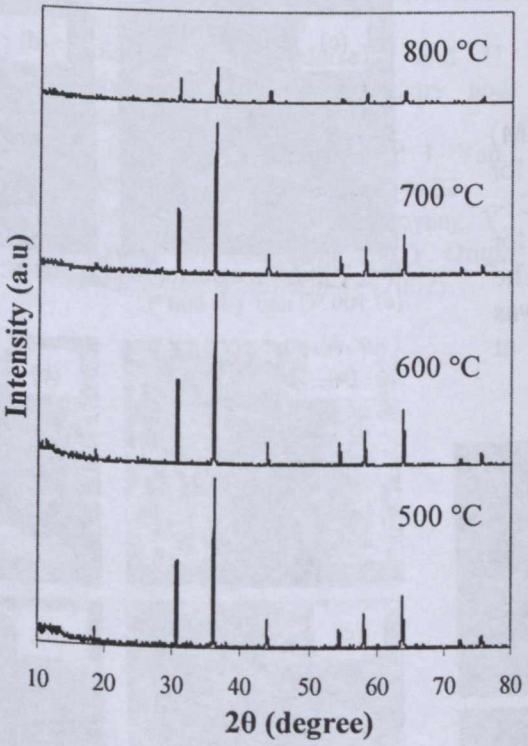

Fig. 3 XRD pattern of V3 calcined at various temperatures

The XRD pattern for V shows that a peak at $2\theta = 8.6°$ which confirms the formation of the $LiNiVO_4$ product that is highly crystalline at [111] ratio of intensity. The position of [220] peak is located at 30.6°. As we expect, the [220] peak is more intense than the [111] peak for inverse spinel [8]. The resulting products for V3 and V8 for all temperatures (500 °C - 800 °C) were clearly showed that each of them was a single phase while for V1 and V2, the mixed phases appear for both compositions. V4, in which Ni is not added, the single phase of the sample was observed to appear at 600 °C and 700 °C. All peaks observed agree with the JCPDS data [9].

The cubic lattice constant, a of sample all samples above can be obtained by using Braggs formula which $a = d\left(h^2 + k^2 + l^2\right)^{1/2}$ where d is the distance between vicinal crystal face and hkl is the Miller index. The change in the scattering angle with x in $LiNi_{1-x}Mn_xVO_4$ is because of the difference of the lattice constants of each compositions although $LiNi_{1-x}Mn_xVO_4$ ($0 \le x \le 1$) have the $LiNiVO_4$ XRD spectra [10].

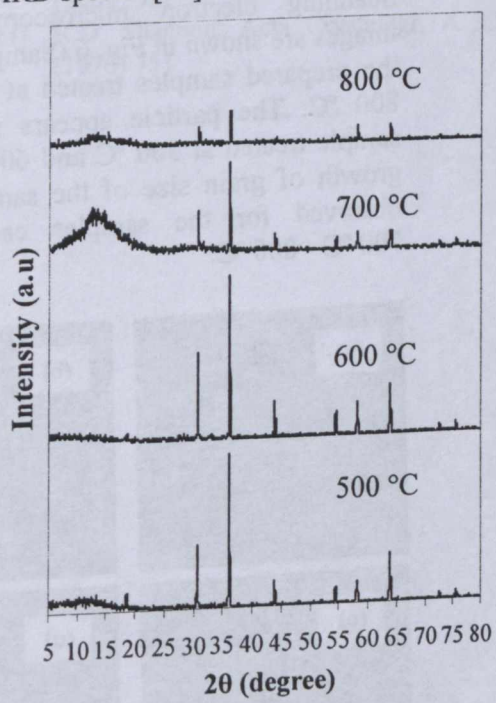

Fig. 4 XRD of V8 calcined at various temperatures

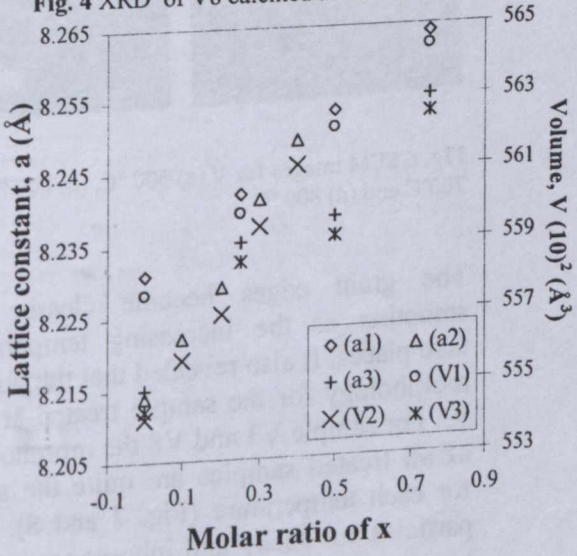

Fig. 5 Lattice constants and volumes of crystal cell for (a1) $LiNi_{1-x}Mn_xVO_4$, (a2) Qiong et al. [6], (a3) $LiNi_{1-x}Mn_xVO_4$ + PEG, (V1) $LiNi_{1-x}Mn_xVO_4$, (V2) Qiong et al. [6] and (V3) $LiNi_{1-x}Mn_xVO_4$ + PEG

From Fig. 5, the lattice constants and the crystal cell volume increased with the increasing amounts of manganese molar ratio in $LiNi_{1-x}Mn_xVO_4$ because the ionic radii of Mn^{2+} is larger than that of Ni^{2+} in the tetrahedral sites and this might be related to the manganese substitution for nickel [11].

3.4 SEM Characterization

Scanning electron microscopy (SEM) images are shown in Fig. 6 (Sample V), for the prepared samples treated at 500 °C – 800 °C. The particle appears sticky for sample treated at 500 °C and 600 °C. The growth of grain size of the samples was observed for the samples calcined at 700 °C - 800 °C.

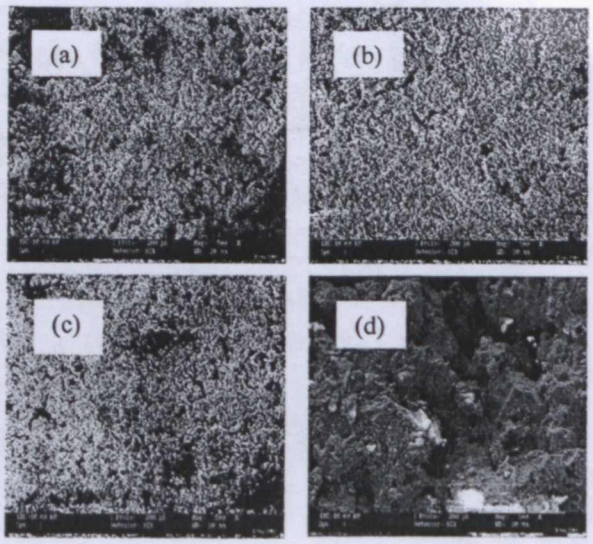

Fig. 6 SEM images for V (a) 500 °C, (b) 600 °C, (c) 700°C and (d) 800 °C

The grain edges became clearer and smoother as the increasing temperature take places. It also revealed that the porous morphology for the sample treated at 800 °C. For sample V3 and V8 the morphology of all treated samples are quite the same for each temperature (Fig. 7 and 8). The particles are sticky and inhomogeneous at lower temperature. As the temperature is increased, the particle started to grow and appeared to have smoother surface and visible grain edges.

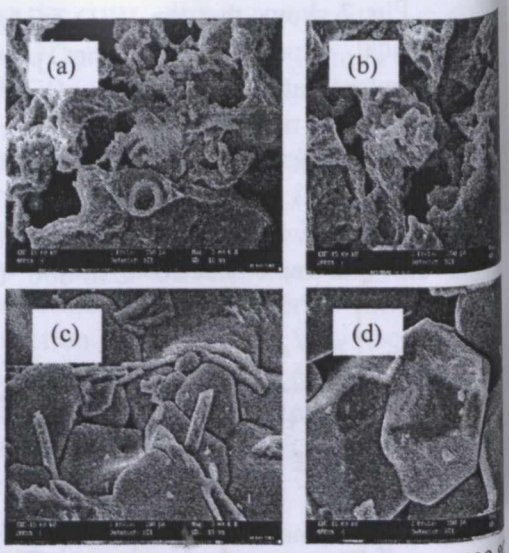

Fig. 7 SEM images for V3 (a) 500 °C, (b) 600 °C (c) 700 °C and (d) 800 °C

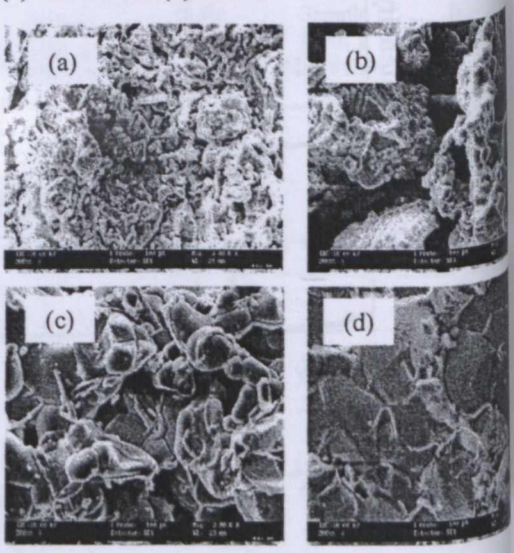

Fig. 8 SEM images for V8 (a) 500 °C, (b) 600 °C (c) 700 °C and (d) 800 °C

4. CONCLUSIONS

The $LiNi_{1-x}Mn_xVO_4$ powders as the cathode materials were successfully prepared by the thermal decomposition of the precursor at 500 °C for 3h ($LiNi_{1-x}Mn_xVO_4$) in air with perfect inverse spinel structure. The grain size of prepared compounds increased as the calcined temperature is increased. The lattice constant was found to increase as the X ratio increases.

REFERENCES

[1] H. Xie and Z. Zhou. Electrochimica Acta 51 (2006) 2063

[2] S. Vivekanandhan, M. Venkateswarlu and N. Satyanarayana. Materials Letters 58 (2004) 1218

[3] A. Subramania, N. Angayarkanni, S.N. Karthick and T. Vasudevan. Materials Letters 60 (2006) 3023

[4] P. Kalyani, N. Kalaiselvi and N. Muniyandi. Materials Chemistry and Physics 77 (2002) 662

[5] Y. Li, Z. Zhou, X. Gao and J. Yan. Electrochimica Acta 52 (2007) 4922

[6] L. Qiongyu, L. Jizheng, J. Xiaoyang, Y. Fangyong, W. Yongqiang and Y. Ding. Chinese Science Bulletin 47 (2002)

[7] J.L. Riu, M. Wang, X. Lin, D.C.Yin and W.D. Huang. J. Power Sources 108 (2002) 113

[8] G.T.K. Fey and W Perng. Materials Chemistry and Physics 47 (1997) 279

[9] Powder diffraction file, Card No. 38-1395, Joint Committee on Powder Diffraction Standards, Swarthmore, PA

[10] Q.Y. Lai, J. Z. Lu, X. B. Su, and X. Yang. J. Solid State Chemistry 165 (2002) 312

[11] R.D. Shannon. Acta Crystalogr. A 32 (1976) 751